

# Clinical and Computed Tomography Characteristics of Solitary Pulmonary Nodules Caused by Fungi: A Comparative Study

Jin Jiang<sup>1,\*</sup>, Zhuo-ma Lv<sup>1,2,\*</sup>, Fa-jin Lv<sup>1</sup>, Bin-jie Fu<sup>1</sup>, Zhang-rui Liang<sup>1</sup>, Zhi-gang Chu<sup>1</sup>

<sup>1</sup>Department of Radiology, The First Affiliated Hospital of Chongqing Medical University, Chongqing, People's Republic of China; <sup>2</sup>Department of Radiology, The Second People's Hospital of Yubei District, Chongqing, People's Republic of China

\*These authors contributed equally to this work

Correspondence: Zhi-gang Chu, Department of Radiology, The First Affiliated Hospital of Chongqing Medical University, 1# Youyi Road, Yuanjiagang, Yuzhong district, Chongqing, 400016, People's Republic of China, Tel +86 18723032809, Fax +86 23 68811487, Email chuzg0815@163.com

**Purpose:** To clarify the clinical and computed tomography (CT) indicators in distinguishing pulmonary nodules caused by fungal infection from lung cancers.

**Methods:** From January 2013 to April 2022, 68 patients with solitary fungal nodules (64 were solid and 4 were mixed ground-glass nodules) and 140 cases with solid cancerous nodules with similar size were enrolled. Their clinical characteristics and CT manifestations of the solid nodules were summarized and compared, respectively.

**Results:** Compared with patients with lung cancers, cases were younger ( $51.2 \pm 11.5$  vs  $61.3 \pm 10.2$  years) and non-smokers (72.1% vs 57.9%) and immunocompromised (44.1% vs 17.9%) individuals were more common in patients with fungal nodules (each  $P < 0.05$ ). The air crescent sign (ACS) (34.4% vs 0%), halo sign (HS) (23.4% vs 4.3%), and satellite lesions (45.3% vs 2.9%) were more frequently detected in fungal nodules than in cancerous ones (each  $P < 0.05$ ). Air bronchogram similarly occurred in fungal and cancerous nodules, whereas the natural ones were more common in the former (100% vs 16.7%,  $P = 0.000$ ). However, the fungal nodules had a lower enhancement degree ( $29.0 \pm 19.2$  HU vs  $40.3 \pm 28.3$  HU,  $P = 0.038$ ) and frequency of hilar and/or mediastinal lymph node enlargement (2.9% vs 14.3%,  $P = 0.013$ ) compared with the cancerous nodules.

**Conclusion:** In the younger, non-smoking and immunocompromised patients, a solitary pulmonary solid nodule with ACS, HS, satellite lesions and/or natural air bronchogram but without significant enhancement, fungal infection is a probable diagnosis.

**Keywords:** tomography, X-ray computed, pulmonary nodules, fungal infection

## Introduction

The widespread application of multislice spiral computed tomography (CT) increases the detection rate of pulmonary nodules which can be divided into solid and subsolid. The subsolid nodules are further divided into pure ground glass nodules (GGNs) (no solid component) and mixed GGNs (both ground-glass and solid components).<sup>1,2</sup> Previous studies have paid more attention to the differential diagnosis of GGNs and had confirmed that the GGNs, especially the mixed ones, had an extremely high probability of being malignant.<sup>3-5</sup> In contrast, the radiological characteristics of the pulmonary solid nodules have not been fully discussed and revealed.<sup>6,7</sup> The aetiology of solid nodules is diverse, comprising tumors, inflammatory disorders, and vascular or congenital causes. Among them, the tumor and inflammatory disease are the most common. Unfortunately, it is usually difficult to correctly differentiate them in clinical practice. Sometimes, the inflammatory nodules are misdiagnosed as malignant tumors, causing unnecessary resection, and vice versa, delaying the best treatment opportunity. In addition, solid cancerous nodules usually grow faster and have a worse prognosis than GGNs.<sup>8,9</sup> Therefore, the differential diagnosis of solid nodules is of greater significance.

Fungal infection is one of the causes of inflammatory lesions, commonly involving the lung and occurs in any population, mainly in immunocompromised patients.<sup>10</sup> The CT manifestations of pulmonary fungal infection vary in patients, including nodules or masses, consolidation and ground glass opacity, which are related to the host's immune status. In immunocompetent patients, the lesions caused by fungal infection were more likely to be single nodular lesions, while those mainly exhibited consolidation and multiple lesions in immunocompromised cases.<sup>11</sup> Compared with multiple fungal nodules, the solitary ones are more likely to be misdiagnosed because they could show the traditional lung cancer features, such as lobulation sign, spiculation sign, air bronchogram, pleural indentation, and vessel convergence.<sup>12,13</sup> Moreover, some of the fungal nodules are stable or even grow up during follow-up.<sup>14</sup> Therefore, it is necessary to distinguish them for better understanding solid nodules.

Cavity, vacuole sign, air crescent sign, halo sign, satellite lesions, and air bronchogram were reported to be commonly detected in pulmonary nodules in patients with fungal infection. However, these signs could also be found in cancerous nodules, while there was no comparative study to verify their diagnostic value for solitary pulmonary fungal nodules.<sup>14–16</sup> Therefore, studies regarding the differential diagnosis between fungal and cancerous nodules are lacking, and fungal nodules are still easily to be misdiagnosed due to uncertainty of clinical and CT features. The aim of this study is to reveal the differences in clinical and CT characteristics between fungal nodules and cancerous ones for better understanding the fungal nodules.

## Materials and Methods

### Patient Selection

This retrospective study was approved by the Institutional Review Board of the First Affiliated Hospital of Chongqing Medical University, and the requirement for informed consent was waived due to the retrospective nature of this study.

From January 2013 to April 2022, consecutive pulmonary fungal nodules and cancerous nodules were retrospectively collected. The inclusion criteria were as follows: 1) the nodules ( $\leq 3$  cm) were pathologically confirmed as fungal infection or lung cancer; 2) complete clinical and CT data were available. The exclusion criteria were as follows: 1) absence of thin-section CT ( $\leq 1$  mm) data; 2) presence of artifacts on CT images affecting evaluation and 3) patients with other concurrent lesions, such as consolidation or ground glass opacity. To eliminate the influence of nodule type and size, the size-matched and solid cancerous nodules were selected for making comparison. Finally, 68 fungal nodules and 140 size-matched solid cancerous nodules were enrolled in the study.

### CT Protocol

Patients were examined using one of the following CT scanners: SOMATOM Perspective (Siemens Healthineers, Erlangen, Germany), SOMATOM Definition Flash (Siemens Healthineers, Erlangen, Germany), or Discovery CT750 HD (GE Healthcare, Milwaukee, WI, USA). To minimize breathing artifact, all CT scans were performed at the end of inspiration, during a single breathhold. The scan range was from the thoracic entrance to the costophrenic angle. Plain CT scan was acquired with the following settings: tube voltage, 110–130 kVp; tube current time, 50–140 mA (using automatic current modulation technology); scanning slice thickness, 5 mm; rotation time, 0.5 s; pitch, 1–1.1; collimation, 0.6 or 0.625 mm; reconstruction slice thickness and interval, 0.625 or 1 mm; matrix, 512×512. All images were reconstructed into 0.625 or 1 mm slice thickness using a standard algorithm or medium-sharp algorithm. All patients underwent plain CT scan, and 115 of them (30 with fungal nodules, 85 with lung cancers) underwent contrast-enhanced CT scan with a total of 80–100 mL of nonionic iodinated contrast material (Iopamidol, 320 mgI/mL; Shanghai Bracco Sine Pharmaceutical Co., Ltd., China) at an injection rate of 3.0 mL/s, followed by 50 mL of saline solution via a power injector. Images were obtained with mediastinal (width, 350–400 HU; level, 20–40 HU) and lung (width, 1200–1600 HU; level, –500 to –700 HU) window settings.

### Clinical Data and Image Analysis

The patients' clinical data were recorded using the Electronic Medical Record System (Winning Health, China). Clinical data, including the patient's gender, age, clinical symptoms (cough, expectoration, fever), smoking history, history of

malignant tumor, history of drinking and immune status (immunocompetent or immunocompromised), which were recorded and evaluated. Immunocompromised patients were those who had long-standing diabetes mellitus, end-stage liver or kidney disease, autoimmune diseases, acquired immune deficiency syndrome, hematologic malignancies, solid organ or hematopoietic stem cell transplantation, idiopathic CD4 lymphocytosis, agranulocytosis, aggressive glucocorticoid or immunosuppressive therapy, and other conditions or treatments resulting in immunodeficiency.<sup>17</sup> All clinical data were collected by the radiologists through the Electronic Medical Record System.

The CT data were analyzed on a picture archiving and communication system workstation (Carestream Vue PACS) with lung window settings (window level, -600 HU; window width: 1500 HU). Two independent and experienced radiologists, who were blinded to the pathological results, analyzed all the CT data, and discordant opinions were resolved by consensus. The characteristics of lesions on both plain and enhanced CT scans were combined.

Based on the previous findings on fungal infection's CT characteristics of fungal infection,<sup>14–16</sup> the cavity, vacuole sign, air crescent sign (ACS), halo sign (HS), satellite lesions, air bronchogram and lymph node enlargement were evaluated for both fungal nodules and cancerous nodules. Besides, the following CT features were also analyzed: nodule size (the mean of the longest diameter and the perpendicular diameter on axial CT images), distribution (upper, lower, or middle lobe), CT value on plain CT scan, and degree of enhancement (peak CT value on contrast-enhanced CT scan - CT value on plain CT scan). Cavity was defined as a lucency within a zone of pulmonary nodule, which may or may not contain a fluid level and had varied thickness.<sup>18</sup> Vacuole sign was defined as round or irregular air attenuation with a diameter of 1–2 mm in a nodule.<sup>19</sup> The ACS was defined as a crescent or half-moon-shaped collection of air in the periphery of an intracavitary nodule or mass, separating the nodule or mass from the cavity wall.<sup>18</sup> HS was defined as ground-glass opacity surrounding a nodule in the lung parenchyma.<sup>18</sup> Satellite lesions were defined as small discrete shadows in the immediate vicinity of the main lesion.<sup>20</sup> Mediastinal and hilar lymph node enlargement was defined as lymph nodes with at least 1-cm short axes.<sup>20</sup> Air bronchogram was defined as a pattern of air-filled (low attenuation) bronchi in the nodule.<sup>18</sup> The presentation of intro-nodular air bronchogram has four types: type I, normal bronchi passing by or through nodules (natural); type II, dilated or distorted bronchi within nodules; type III, truncated within nodules, and type IV, dilated and truncated within nodules.

## Statistical Analysis

The patients' clinical data and nodules' CT features of nodules were statistically analyzed using the SPSS software package (version 26.0, IBM, NY, USA). Continuous variables were expressed as mean  $\pm$  standard deviation, and categorical variables were expressed as number and percentage. To compare variable differences in variables between fungal nodules and cancerous nodules, the analysis of variance was used for patients' age, and the Mann-Whitney *U*-test was used for density, and degree of enhancement and the Pearson chi-square test or Fisher's exact test was used for sex, history of cancer, smoking history, drinking history, lesion location, respiratory symptoms, immune status and different CT features' frequencies. A *P*-value of  $<0.05$  was considered to indicate a statistically significant difference.

## Results

### Patients' Clinical Characteristics

Among the 68 fungal nodules, 64 (94.1%) were solid and 4 (5.9%) were mGGNs, and 38 (55.9%), 29 (42.6%) and 1 (1.5%) were caused by cryptococcus, aspergillus, and mucormycosis, respectively. The 140 solid cancerous nodules included 114 (81.4%) invasive adenocarcinoma, 13 (9.3%) squamous cell carcinoma, 4 (2.9%) adenocarcinoma in situ, 6 (4.3%) minimally invasive adenocarcinoma, 1 (0.7%) atypical carcinoid, 1 (0.7%) small cell lung cancer, and 1 (0.7%) adenosquamous carcinoma. [Table 1](#) summarizes the patients' clinical characteristics. Compared with patients with lung cancers, cases were younger ( $P = 0.000$ ) and non-smokers ( $P = 0.047$ ) and immunocompromised ( $P = 0.000$ ) individuals in whom fungal nodules were more common.

**Table 1** Patients' Clinical Characteristics

Characteristics	Patients with Fungal Nodules (n = 68)	Patients with Cancerous Nodules (n = 140)	P-value
Age (years)	51.2 ± 11.5	61.3 ± 10.2	0.000
Sex (male)	37 (54.4)	78 (55.7)	0.859
History of malignant tumor	7 (10.3)	10 (7.1)	0.436
Number of immunocompromised cases	30 (44.1)	25 (17.9)	0.000
Smoking history	19 (27.9)	59 (42.1)	0.047
Drinking history	18 (26.5)	41 (29.3)	0.673
Clinical symptoms	30 (44.1)	75 (53.6)	0.201

**Note:** Data are expressed as number (percentage) or mean ± standard deviation.

## CT Features of PSNs

The fungal and cancerous nodules' CT characteristics are summarized in [Table 2](#). The ACS was only detected in fungal nodules ([Figure 1](#)). Air bronchogram occurrences in nodules were similar between these two groups, while the natural one was more common in fungal nodules ( $P = 0.000$ ) ([Figure 2](#)). The HS was more frequent in fungal nodules than in the cancerous ones ( $P = 0.000$ ), especially the annular and ill-defined one ( $P = 0.000$ ) ([Figures 2–3](#)). Satellite lesions were also more common in fungal nodules ( $P = 0.000$ ) ([Figure 4](#)), whereas the hilar and/or mediastinal lymph nodule enlargement was less commonly detected in them. On plain CT images, the density of fungal nodules was higher than that of the cancerous ones, but their degree of enhancement was lower (each  $P < 0.05$ ). On enhanced CT images, 5 (16.7%) fungal nodules had no enhancement ([Figure 5](#)). Among the 68 fungal nodules, 12 (17.6%) had no above mentioned morphological signs, which were significantly smaller than those with these features ( $0.9 \pm 0.2$  vs  $1.6 \pm$

**Table 2** CT Characteristics of the Fungal and Cancerous Nodules

Characteristics	Fungal Nodules (n = 68)	Cancerous Nodules (n = 140)	P-value
Size (cm)	1.5 ± 0.7	1.5 ± 0.6	0.696
Distribution			0.647
Upper lobe	41 (60.3)	89 (63.6)	
Middle and lower lobe	27 (39.7)	51 (36.4)	
ACS	22 (34.4)	0 (0.00)	0.000
Vacuole sign	6 (9.4)	7 (5.0)	0.380
HS	15 (23.4)	6 (4.3)	0.000
Annular and ill-defined HS	11 (73.3)	0 (0.00)	0.000
Annular and well-defined HS	1 (6.7)	0 (0.00)	
Partial and well-defined HS	3 (20.0)	6 (100.0)	
Air bronchogram	12 (18.8)	30 (21.4)	0.661
Type I	12 (100)	5 (16.7)	0.000
Type II	0	4 (13.3)	
Type III	0	20 (66.7)	
Type IV	0	1 (2.4)	
Cavity	3 (4.7)	6 (4.3)	0.897
Satellite lesions	29 (45.3)	4 (2.9)	0.000
Lymph node enlargement	2 (2.9)	20 (14.3)	0.013
Plain CT value (HU)	33.7 ± 31.3	22.5 ± 20.8	0.014
Enhanced CT value (HU)	62.7 ± 30.9	62.8 ± 31.3	0.493
ΔCT value (HU)	29.0 ± 19.2	40.3 ± 28.3	0.038

**Note:** Data are expressed as number (percentage) or mean ± standard deviation.

**Abbreviations:** ACS, air crescent sign; HS, halo sign; ΔCT value, degree of enhancement.

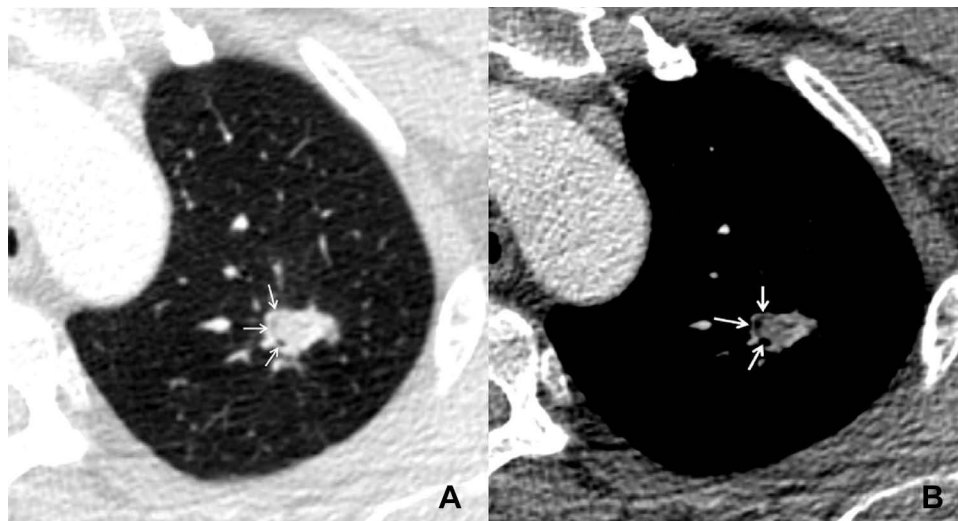


**Figure 1** A patient with pulmonary cryptococcosis. (A and B) axial CT images show a solid nodule located in the left upper lobe, there is a crescent-shaped collection of air and lower density in the periphery of this nodule (air crescent sign) (arrows). (B) on enhanced CT image, the nodule shows ring-like enhancement.

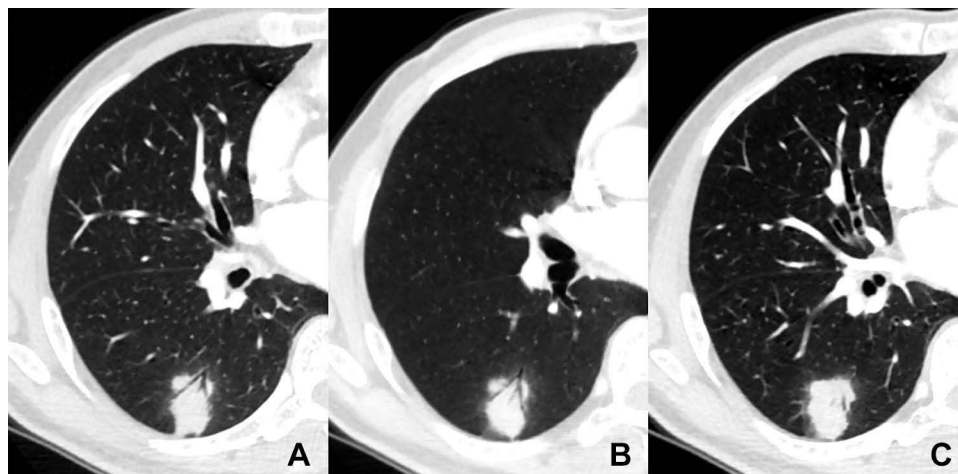


**Figure 2** A patient with diabetes and pulmonary cryptococcosis. (A) axial and (B) minimum intensity projection images show a solid nodule located in the right lower lobe. There are multiple natural bronchi in it. (C) axial CT image shows that the nodule is surrounded by annular and ill-defined ground glass opacity (halo sign).

0.6 cm,  $P = 0.000$ ). The four mGGNs caused by fungal infection were all ill-defined, and three of them were regular, the internal solid component in one and three was strip-shaped and scattered, respectively.

## Discussion

The solitary pulmonary nodules, those caused by fungal infection are relatively uncommon and their CT characteristics are not well understood and are frequently misdiagnosed as tumors in clinical practice, leading to unnecessary surgical resection. Therefore, further understanding fungal and malignant nodule differences is very important. The present study determined some differences in clinical and CT characteristics between fungal and cancerous nodules. The fungal nodules were more likely to be found in younger and immunocompromised patients, and more cases had ACS, natural air bronchogram, annular and ill-defined HS and satellite lesions on CT images. In contrast, cancerous nodules were more commonly detected in smokers and older individuals, and more cases had bronchial truncation and/or dilation, partial and well-defined HS, and hilar and mediastinal lymph node enlargement. Additionally, fungal nodules had lower degree of enhancement than that of cancerous ones. These specific differences in clinical and CT features were important in differentiating fungal nodules from cancerous ones.

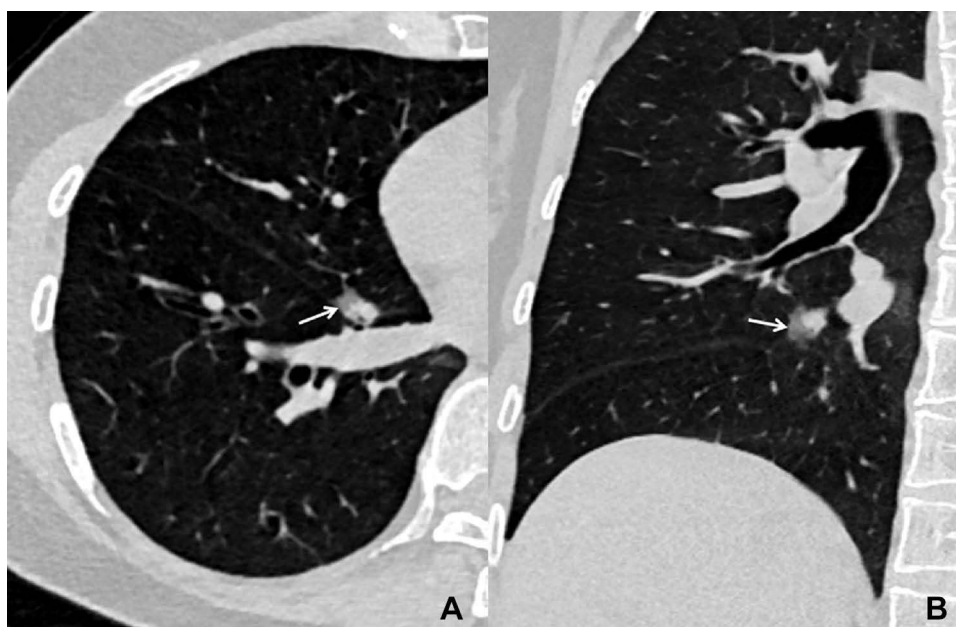


**Figure 3** A patient with invasive adenocarcinoma. (A) axial and coronal (B) CT images show a solid nodule located in the right middle lobe, and there is partial and well-defined ground glass opacity (halo sign) in its periphery (arrow).

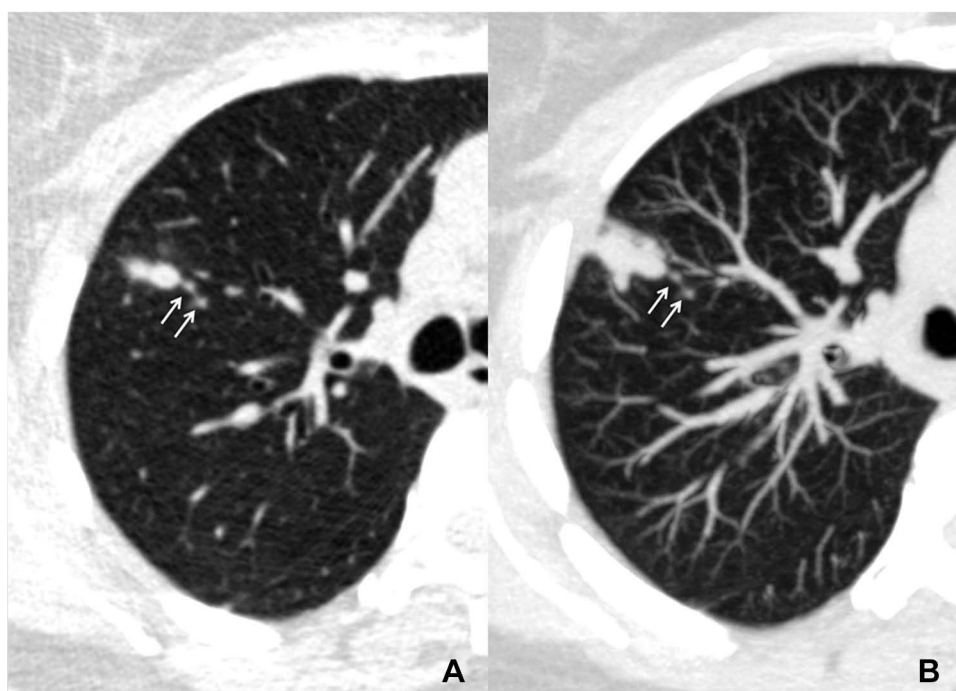


**Figure 4** A patient with pulmonary cryptococcosis. (A) axial and (B) maximum intensity projection images show a solid nodule located in the right upper lobe. There are multiple scattered smaller nodules (satellite lesions, arrows) in the adjacent lung field.

The incidence of lung cancer is associated with age and smoking history because the immunity usually decreased along with age but the total exposure to carcinogens increased with smoking years.<sup>21,22</sup> In the immunocompromised patients, the body does not produce a strong immune response and enough cytokine against infection, thus increasing the chance of fungal infection.<sup>17</sup> In this study, significantly more patients with fungal nodules were immunocompromised, which was identical to previous result.<sup>23</sup> Thus, age, smoking history and immune status should be considered and

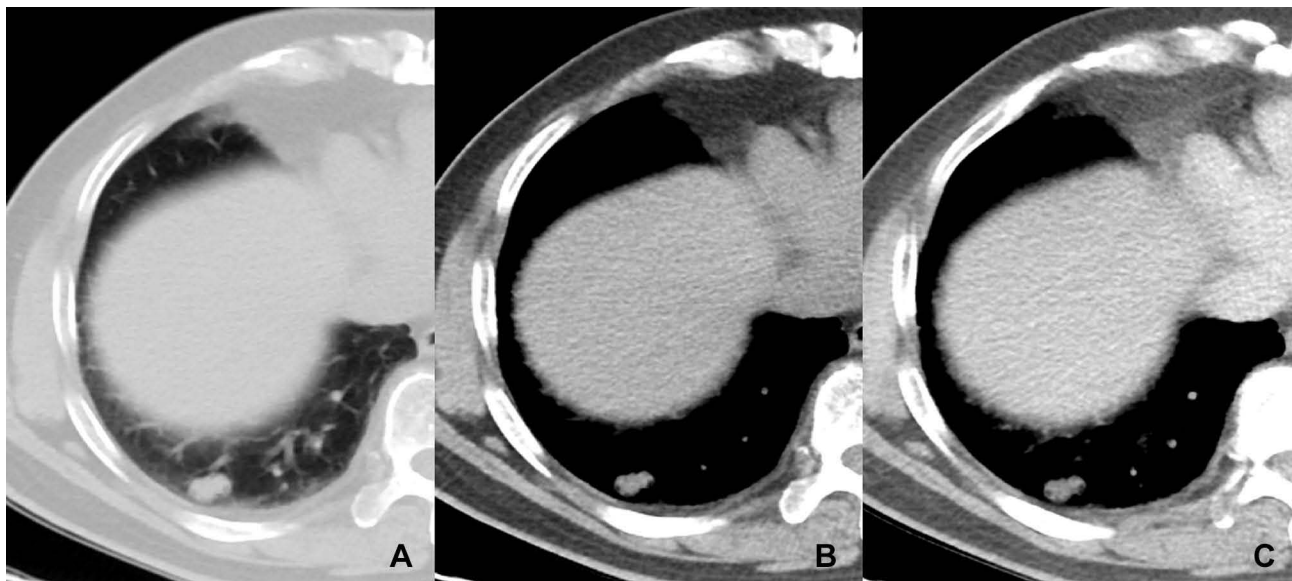


**Figure 5** A patient with a history of diabetes mellitus for 15 years and pulmonary aspergillus. (A and B) axial plain CT images show an oval and well-defined solid nodule located in the right lower lobe (CT value = 14HU). On enhanced CT image (C), it has no significant enhancement (CT value = 15HU).

evaluated for differentiating pulmonary nodules, and fungal infection should be considered as one cause of nodules in the immunocompromised patients without high risk factors of lung cancer.

The ACS was usually seen in aspergillosis, which correlated histopathologically with the areas of the hypha form of pulmonary vasculature resulting in pulmonary hemorrhage, arterial thrombosis, and eventual lung infarction.<sup>24</sup> It was formed by retraction of the infarct centre and resorption of necrotic tissue by leukocytes, which occurred first in the periphery and then gradually extended to the central region.<sup>16</sup> However, the ACS must be related to the clinical setting of underlying disease because this sign was not only seen in aspergilloma but also in other fungal infections.<sup>24</sup> In our study, the ACS only occurred in fungal nodules and most of the residual solid components had no or slight enhancement. Therefore, this sign may be specific for distinguishing fungal nodules from lung cancer, which should be paid more attention in differentiating nodules.

The HS is highly indicative of an angioinvasive fungal infection, which is also commonly seen in aspergillosis.<sup>25</sup> Pathologically, it is caused by accumulation of inflammatory cells and exudation in the central zone and spreading to the surrounding lung tissue.<sup>26</sup> In the present study, both the fungal nodules and lung cancers had this sign but which was more common in the former and had significantly different CT characteristics between them. The HS in fungal nodules was usually annular and ill-defined, while all of that in lung cancers was partial and well-defined, which was consistent with previous results.<sup>26,27</sup> Therefore, the HS should be seen as another key radiological indicator in differentiating them; however, its boundary and scope should be further evaluated before making diagnosis.

Satellite lesions were small discrete shadows in the main lesion immediate vicinity.<sup>20</sup> They were usually found in infectious lesions, especially pulmonary tuberculosis, but also in malignant lesions, indicating benign or metastatic.<sup>28</sup> In the present study, satellite lesions were also more common in fungal nodules but rare in cancerous ones, which was consistent with previous results.<sup>29</sup> However, fungal nodules and tuberculosis may share some CT features, and some of which could not be easily differentiated. The reason for this resemblance is that both diseases are basically granulomatous inflammation, which produces endobronchially spread nodules.<sup>30</sup> Thus, for a solid nodule with satellite lesions, fungal infection should be suspected, but further differentiation from pulmonary tuberculosis is required.

Air bronchogram can be detected in both benign and malignant nodules. The former is due to inflammatory response composed of histiocytes, multinucleated giant cells and lymphocytic infiltration without destruction of tissue architecture, while the latter may be related to the invasiveness of tumor cells. In the present study, it was found that the air bronchogram occurrences between these two groups were similar, while bronchial truncation and/or dilatation occurred

only in cancerous nodules. Hence, fungal nodules should be suspected if the internal bronchus was natural, whereas lung cancer should be firstly considered if nodules had bronchial truncation and/or dilation.

Lymph node enlargement is usually caused by the invasion or propagation of either inflammatory cells or neoplastic cells into the node.<sup>31</sup> It was revealed that focal inflammatory lesions usually caused hilar lymph node enlargement, while simultaneous hilar and mediastinal lymph node enlargement was usually found in lung cancers due to metastasis.<sup>32</sup> In the present study, lymph node enlargement was more common in lung cancer than in fungal nodules, especially the simultaneous hilar and mediastinal lymph node enlargement. Therefore, in patients with solid nodules and significant lymph node enlargement, lung cancer should be taken into consideration.

The density of fungal nodules was higher than that of cancerous ones on plain CT scan because fungal infection could result in a large number of inflammatory cell infiltration inside the lesion. In contrast to the anastomosing vascular pools and vascular lakes formed in lung cancers, inflammatory cell infiltration and vasculitis led to coagulative necrosis in fungal nodules, causing lower enhancement or even no enhancement.<sup>33,34</sup> However, some active fungal nodules had no significant necrosis, they may also exhibit obvious enhancement, which overlaps with the enhanced characteristics of lung cancers. Thus, only a solid nodule without significant enhancement may indicate fungal infection.

Part solid nodules have been reported to be associated with lung adenocarcinoma, and its malignancy rate was higher than that of pGGNs or solid nodules. It has been reported that well-defined border and heterogeneous GGO, and multiple, irregular, scattered, and eccentric internal solid components were significant indicators of malignant mGGNs, while ill-defined border and homogeneous GGO, and single, round and central internal solid components were predictors of benign ones.<sup>35</sup> In this study, the four mGGNs caused by fungal infection were ill-defined and the internal solid components were irregular or scattered, which did not meet the typical features of benign or malignant ones and thus may be misdiagnosed. In view of the nature of infection, short-term follow-up may provide some additional information in differentiating them. In this study, the internal solid components in one mGGN significantly increased after 1 month. Thus, when a mGGN is characterized by significant changes in a short-term, fungal infections should be considered as one of the differential diagnosis.

Our study had some limitations. First, the number of patients with fungal nodules in this study is relatively small. Second, histopathological examination can confirm a definite diagnosis of fungal infection but cannot identify the specific species due to no microbial culture. Third, not all the patients with fungal nodules had enhanced CT data. Thus, the current findings on fungal nodules should be verified in the further studies. Fourth, some fungal nodules cannot be diagnosed because they had none of the above mentioned features. It may be because only when they are large enough can they exhibit these CT features. For the smaller ones, further study is needed for differentiation.

## Conclusion

In conclusion, the solid fungal nodules and cancerous ones exhibit different clinical and CT characteristics. The younger and immunocompromised individuals were more common in patients with fungal nodules than patients with lung cancers. On CT images, fungal nodules frequently show ACS, annular and ill-defined HS, satellite lesions, natural air bronchogram, and lower enhancement, whereas partial and well-defined HS, bronchial truncation and/or dilation, and simultaneous hilar and mediastinal lymph node enlargement are commonly detected in lung cancers. In the younger, non-smoking and immunocompromised patients, fungal infection is a probable diagnosis for a solitary pulmonary solid nodule with ACS, HS, satellite lesions and/or natural air bronchogram but without significant enhancement.

## Ethics Statement

The study was conducted in accordance with the Declaration of Helsinki, and the protocol was approved by the Ethics Committee of the First Affiliated Hospital of Chongqing Medical University (No. 2019-062), which absolved the need for written informed consent because of the retrospective study. All personal identification data were anonymized and de-identified before analysis.

## Consent for Publication

All of the images, tables and recordings can be published.

## Funding

This work was supported by the Joint Project of Chongqing Science and Technology Commission and Chongqing Public Health Commission (2022MSXM050) and the Senior Medical Talents Program of Chongqing for Young and Middle-aged from Chongqing Health Commission (Receptor: Zhi-gang Chu).

## Disclosure

All authors declare no conflicts of interest for this work.

## References

1. Heuvelmans MA, Walter JE, Peters RB, et al. Relationship between nodule count and lung cancer probability in baseline CT lung cancer screening: the Nelson study. *Lung Cancer*. 2017;113:45–50. doi:10.1016/j.lungcan.2017.08.023
2. Mazzone PJ, Lam L. Evaluating the patient with a pulmonary nodule: a review. *JAMA*. 2022;327(3):264–273. doi:10.1001/jama.2021.24287
3. Fu BJ, Lv FJ, Li WJ, Lin RY, Zheng YN, Chu ZG. Significance of intra-nodular vessel sign in differentiating benign and malignant pulmonary ground-glass nodules. *Insights Imaging*. 2021;12(1):65. doi:10.1186/s13244-021-01012-7
4. Qiu ZX, Cheng Y, Liu D, et al. Clinical, pathological, and radiological characteristics of solitary ground-glass opacity lung nodules on high-resolution computed tomography. *Ther Clin Risk Manag*. 2016;12:1445–1453. doi:10.2147/TCRM.S110363
5. Hu H, Wang Q, Tang H, Xiong L, Lin Q. Multi-slice computed tomography characteristics of solitary pulmonary ground-glass nodules: differences between malignant and benign. *Thorac Cancer*. 2016;7(1):80–87. doi:10.1111/1759-7714.12280
6. Feng B, Chen X, Chen Y, et al. Solitary solid pulmonary nodules: a CT-based deep learning nomogram helps differentiate tuberculosis granulomas from lung adenocarcinomas. *Eur Radiol*. 2020;30(12):6497–6507. doi:10.1007/s00330-020-07024-z
7. Perandini S, Soardi G, Motton M, Oliboni E, Zantedeschi L, Montemezzi S. Distribution of solid solitary pulmonary nodules within the lungs on Computed Tomography: a review of 208 consecutive lesions of Biopsy-Proven nature. *Pol J Radiol*. 2016;81:146–151. doi:10.12659/PJR.895417
8. Miura K, Hamanaka K, Koizumi T, Kawakami S, Kobayashi N, Ito KI. Solid component tumor doubling time is a prognostic factor in non-small cell lung cancer patients. *J Cardiothorac Surg*. 2019;14(1):57. doi:10.1186/s13019-019-0879-x
9. Chen C, Huang X, Peng M, Liu W, Yu F, Wang X. Multiple primary lung cancer: a rising challenge. *J Thorac Dis*. 2019;11(Suppl 4):S523–S536. doi:10.21037/jtd.2019.01.56
10. Rotjanapan P, Chen YC, Chakrabarti A, et al. Epidemiology and clinical characteristics of invasive mould infections: a multicenter, retrospective analysis in five Asian countries published correction appears in *Med Mycol*. 2018 Apr 1; 56(3):387. *Med Mycol*. 2018;56(2):186–196. doi:10.1093/mmy/myx029
11. Wang DX, Zhang Q, Wen QT, et al. Comparison of CT findings and histopathological characteristics of pulmonary cryptococcosis in immunocompetent and immunocompromised patients. *Sci Rep*. 2022;12(1):5712. doi:10.1038/s41598-022-09794-6
12. Jones GS, Baldwin DR. Recent advances in the management of lung cancer. *Clin Med*. 2018;18(Suppl 2):s41–s46. doi:10.7861/clinmedicine.18-2-s41
13. Yanagawa M, Tsubamoto M, Satoh Y, et al. Lung adenocarcinoma at CT with 0.25-mm section thickness and a 2048 matrix: high-spatial-resolution imaging for predicting invasiveness. *Radiology*. 2020;297(2):462–471. doi:10.1148/radiol.2020201911
14. Chen F, Liu YB, Fu BJ, Lv FJ, Chu ZG. Clinical and Computed Tomography (CT) characteristics of pulmonary nodules caused by cryptococcal infection. *Infect Drug Resist*. 2021;14:4227–4235. doi:10.2147/IDR.S330159
15. Suwatanapongched T, Visoottiviseth Y, Watcharananan SP, Kanoksil W, Muntham D, Pornsuriyasak P. Clinical characteristics and CT manifestations of invasive pulmonary aspergillosis in hospitalised patients with systemic lupus erythematosus. *Clin Radiol*. 2021;76(7):548.e13–548.e23. doi:10.1016/j.crad.2021.01.006
16. Nam BD, Kim TJ, Lee KS, Kim TS, Han J, Chung MJ. Pulmonary mucormycosis: serial morphologic changes on computed tomography correlate with clinical and pathologic findings. *Eur Radiol*. 2018;28(2):788–795. doi:10.1007/s00330-017-5007-5
17. Wang Y, Gu Y, Shen K, et al. Clinical features of cryptococcosis in patients with different immune statuses: a multicenter study in Jiangsu Province-China. *BMC Infect Dis*. 2021;21(1):1043. doi:10.1186/s12879-021-06752-x
18. Hansell DM, Bankier AA, MacMahon H, McLoud TC, Müller NL, Remy J. Fleischner Society: glossary of terms for thoracic imaging. *Radiology*. 2008;246(3):697–722. doi:10.1148/radiol.2462070712
19. Fan L, Liu SY, Li QC, Yu H, Xiao XS. Pulmonary malignant focal ground-glass opacity nodules and solid nodules of 3 cm or less: comparison of multi-detector CT features. *J Med Imaging Radiat Oncol*. 2011;55(3):279–285. doi:10.1111/j.1754-9485.2011.02265.x
20. Shi W, Zhou L, Peng X, et al. HIV-infected patients with opportunistic pulmonary infections misdiagnosed as lung cancers: the clinicoradiologic features and initial application of CT radiomics. *J Thorac Dis*. 2019;11(6):2274–2286. doi:10.21037/jtd.2019.06.22
21. Barta JA, Powell CA, Wisnivesky JP. Global epidemiology of lung cancer. *Ann Glob Health*. 2019;85(1):8. doi:10.5334/aogh.2419
22. Xiao YD, Lv FJ, Li WJ, Fu BJ, Lin RY, Chu ZG. Solitary pulmonary inflammatory nodule: CT features and pathological findings. *J Inflamm Res*. 2021;14:2741–2751. doi:10.2147/JIR.S304431
23. Welte T, Len O, Muñoz P, Romani L, Lewis R, Perrella A. Invasive mould infections in solid organ transplant patients: modifiers and indicators of disease and treatment response. *Infection*. 2019;47(6):919–927. doi:10.1007/s15010-019-01360-z
24. Sevilha JB, Rodrigues RS, Barreto MM, Zanetti G, Hochegger B, Marchiori E. Infectious and non-infectious diseases causing the air crescent sign: a state-of-the-Art review. *Lung*. 2018;196(1):1–10. doi:10.1007/s00408-017-0069-3
25. Greene RE, Schlamm HT, Oestmann JW, et al. Imaging findings in acute invasive pulmonary aspergillosis: clinical significance of the halo sign. *Clin Infect Dis*. 2007;44(3):373–379. doi:10.1086/509917
26. Lin RY, Lv FJ, Fu BJ, Li WJ, Liang ZR, Chu ZG. Features for predicting absorbable pulmonary solid nodules as depicted on Thin-Section Computed Tomography. *J Inflamm Res*. 2021;14:2933–2939. doi:10.2147/JIR.S318125

27. Chu ZG, Zhang Y, Li WJ, Li Q, Zheng YN, Lv FJ. Primary solid lung cancerous nodules with different sizes: computed tomography features and their variations. *BMC Cancer*. 2019;19(1):1060. doi:10.1186/s12885-019-6274-0
28. Totanarunroj K, Chaopotong S, Tongdee T. Distinguishing small primary lung cancer from pulmonary tuberculoma using 64-slices multidetector CT. *J Med Assoc Thai*. 2012;95(4):574–582.
29. Liu SQ, Ma XB, Song WM, et al. Using a risk model for probability of cancer in pulmonary nodules. *Thorac Cancer*. 2021;12(12):1881–1889. doi:10.1111/1759-7714.13991
30. Murayama S, Sakai S, Soeda H, et al. Pulmonary cryptococcosis in immunocompetent patients: HRCT characteristics. *Clin Imaging*. 2004;28(3):191–195. doi:10.1016/S0899-7071(03)00145-1
31. Bazemore AW, Smucker DR. Lymphadenopathy and malignancy. *Am Fam Physician*. 2002;66(11):2103–2110.
32. Chu ZG, Sheng B, Liu MQ, Lv FJ, Li Q, Ouyang Y. Differential diagnosis of solitary pulmonary inflammatory lesions and peripheral lung cancers with contrast-enhanced Computed Tomography. *Clinics*. 2016;71(10):555–561. doi:10.6061/clinics/2016(10)01
33. Wang D, Wu C, Gao J, et al. Comparative study of primary pulmonary cryptococcosis with multiple nodules or masses by CT and pathology. *Exp Ther Med*. 2018;16(6):4437–4444. doi:10.3892/etm.2018.6745
34. Li CR, Li YZ, Li YM, Zheng YS. Dynamic and contrast enhanced CT imaging of lung carcinoma, pulmonary tuberculoma, and inflammatory pseudotumor. *Eur Rev Med Pharmacol Sci*. 2017;21(7):1588–1592.
35. Li WJ, Lv FJ, Tan YW, Fu BJ, Chu ZG. Benign and malignant pulmonary part-solid nodules: differentiation via thin-section computed tomography. *Quant Imaging Med Surg*. 2022;12(1):699–710. doi:10.21037/qims-21-145

## Infection and Drug Resistance

Dovepress

### Publish your work in this journal

Infection and Drug Resistance is an international, peer-reviewed open-access journal that focuses on the optimal treatment of infection (bacterial, fungal and viral) and the development and institution of preventive strategies to minimize the development and spread of resistance. The journal is specifically concerned with the epidemiology of antibiotic resistance and the mechanisms of resistance development and diffusion in both hospitals and the community. The manuscript management system is completely online and includes a very quick and fair peer-review system, which is all easy to use. Visit <http://www.dovepress.com/testimonials.php> to read real quotes from published authors.

Submit your manuscript here: <https://www.dovepress.com/infection-and-drug-resistance-journal>